(図 3)

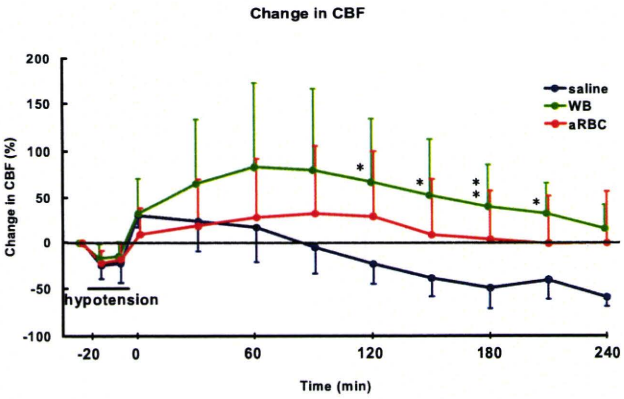


5 時間後まで死亡例はなく、2 例は覚醒し、1 例は 1 週間以上生存した（図 4)。

(図 4)

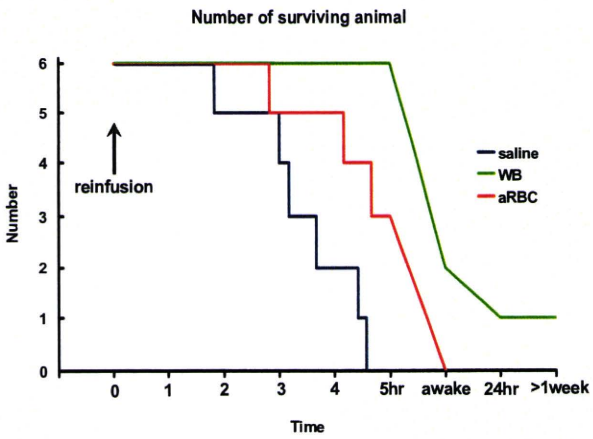


人工赤血球を投与すると、血圧の変化は生食群、全血群の中間のレベル（図 1）であった。PO2（図 2）と CBF（図 3）は一過性の上昇が認められず、ベースに近いレベルを維持した。5 時間後まで半数が生存したが（図 4)、覚醒することはなかった。

脱血により PaO2 は 92.2±10.0 mmHg から 113.2 ±8.0 mmHg に上昇、PaCO2 は 40.3±4.8 mmHg から 33.9±4.2 mmHg に低下、Hct は 46.3±2.4 %から 37.5±3.5 %に低下し、いずれも 3 群間で有意な差はなかった。生食の酸素分圧は 186.3±5.9 mmHg であり、生食の投与によって PaO2 は高いレベルに維持されたが、PaCO2 は低レベルのままであった。全血の投与によって PaO2 はほぼ脱血前のレベルを維持し、PaCO2 は上昇した。人工赤血球懸濁液の酸素分圧は生食に近い 194.5±12.8 mmHg であったが、投与後の PaO2 は全血の場合と同様に脱血前に近いレベルに回復し、PaCO2 は全血の場合より有意に小さい変化であった。Hct は生食投与群では低レベルのままであったが、人工赤血球の投与によって全血投与群よりは低いものの脱血前に近いレベルを維持した（図 5)。

(図 5)

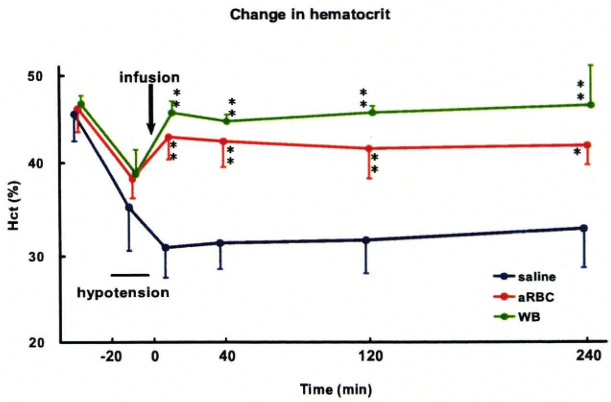


血中電解質濃度 (Na+、K+) および pH はいずれも 3 群間で有意な差はなかった。

## D. 結論

生理学的パラメーター、脳表酸素分圧、脳血流、生存率などを解析することにより、脱血後に人工赤血球を投与した場合の効果について、より詳細な情報が得られた。出血性ショックの際に、人工赤血球投与が少なくとも一時的には延命効果があることを示唆しており、既に報告した *in vivo* 脳微小循環動態の結果と併せ、さらなるデータの蓄積・検討が必要である。

参考文献

1- Sakai H. Tsuchida E, Horinouchi H, Kobayashi K. One-year observation of Wistar rats after intravenous infusion of hemoglobin-vesicles (artificial oxygen carriers). Artificial Cells, Blood Substitutes, and Biotechnology. 2007. 35: 81-91.

2- Tomita Y, Kubis N, Calando Y, Tran Dinh A, Meric P, Seylaz J, Pinard E. Long-term *in vivo* investigation of mouse cerebral microcirculation by fluorescence confocal microscopy in the area of focal ischemia. J Cereb Blood Flow Metab. 2005. 25: 858-867.

3- Rivière C, Martina MS, Tomita Y, Wilhelm C, Tran Dinh A, Ménager C, Pinard E, Lesieur S, Gazeau F, Seylaz J. Magnetic targeting of nanometric magnetic fluid loaded liposomes to specific brain intravascular areas: a dynamic imaging study in mice. Radiology. 2007. 244: 439-448.

4- Tran Dinh A, Kubis N, Tomita Y, Karaszewski B, Calando Y, Oudina K, Petite H, Seylaz J, Pinard E. *In vivo* imaging with cellular resolution of bone marrow cells transplanted into the ischemic brain of a mouse. Neuro Image. 2006. 31: 958-968.

5- Kubis N, Tomita Y, Planat V, Tran Dinh A, Planat-Bernard V, André M, Karaszewski B, Waekel L, Pénicaud L, Silvestre J-S, Casteilla L, Seylaz J, Pinard E. Vascular fate of adipose tissue-derived adult stem cells in the ischemic murine brain : an *in vivo* imaging study. Neuro Image. 2007. 34: 1-11.

6- Tomita Y, Pinard E, Tran-Dinh A, Schiszler I, Kubis N, Tomita M, Suzuki N, Seylaz J. Long-term, repeated measurements of mouse cortical microflow at the same region of interest with high spatial resolution. Brain Res. 2011. 1372: 59-69.

## E. 健康危険情報

該当なし

## F. 研究発表

### 1. 主な論文発表

1. Tomita M, Osada T, Unekawa M, Tomita Y, Toriumi H, Suzuki N. Exogenous nitric oxide increases microflow but decreases RBC attendance in single capillaries in rat cerebral cortex. Microvasc. Rev. Commun. 2010. 3(1): 11-16.
2. Unekawa M, Tomita M, Tomita Y, Toriumi H, Miyaki K, Suzuki N. RBC velocities in single capillaries of mouse and rat brains are the same, despite 10-fold difference in body size. Brain Res. 2010. 1320: 69-73.
3. Miyaki K, Oo T, Song Y, Lwin H, Tomita Y, Hoshino H, Suzuki N, Muramatsu M. Association of a cyclin-dependent kinase 5 regulatory subunit-associated protein 1-like 1 (CDKAL1) polymorphism with elevated hemoglobin $A_1$(c) levels and the prevalence of metabolic syndrome in Japanese men: interaction with dietary energy intake. Am J Epidemiol. 2010. 1;172(9): 985-91.
4. Tomita Y, Pinard E, Tran-Dinh A, Schiszler I, Kubis N, Tomita M, Suzuki N, Seylaz J. Long-term, repeated measurements of mouse cortical microflow at the same region of interest with high spatial resolution. Brain Res. 2011. 1372: 59-69.
5. Toriumi H, Shimizu T, Shibata M, Unekawa M, Tomita Y, Tomita M, Suzuki N. Developmental and circulatory profile of the diploic veins. Microvasc Res. 2011. 81: 97-102.
6. Tomita M, Tomita Y, Unekawa M, Toriumi H, Suzuki N. Oscillating neuro-capillary coupling during cortical spreading depression as observed by tracking of FITC-labeled RBCs in single capillaries. NeuroImage. *in press*.

7. Guo H, Itoh Y, Toriumi H, Yamada S, Tomita Y, Hoshino H, Suzuki N. Capillary remodeling and collateral growth without angiogenesis after unilateral common carotid artery occlusion in mice. Microcirculation. *in press*.

## 2. 主な学会発表

(国内学会)

1. 第 38 回日本頭痛学会総会 (東京), 2010/11/19~20 (口演). 畝川美悠紀, 冨田裕, 鳥海春樹, 鈴木則宏. $K^+$による大脳皮質性拡延性抑制誘発反応に対する慢性トピラマート投与の影響.

2. 第 22 回日本脳循環代謝学会総会 (大阪), 2010/11/26~27 (口演). 畝川美悠紀, 冨田稔, 冨田裕, 鳥海春樹, 菅野巌, 鈴木則宏. $K^+$による大脳皮質性拡延性抑制誘発時の毛細血管内赤血球速度および脳波に対する持続的効果.

3. 第 22 回日本脳循環代謝学会総会 (大阪), 2010/11/26~27 (口演). 鳥海春樹, 正本和人, 冨田裕, 畝川美悠紀, 田桑弘之, 伊藤義彰, 菅野巌, 鈴木則宏. マウス中大脳動脈閉塞モデルにおける虚血周辺領域の微小血管およびアストロサイトの経時的形態観察.

4. 第 22 回日本脳循環代謝学会総会 (大阪), 2010/11/26~27 (口演). 正本和人, 冨田裕, 田桑弘之, 畝川美悠紀, 鳥海春樹, 小畠隆行, 鈴木則宏, 菅野巌. マウス大脳皮質における微小血管－アストログリア構造の長期追跡イメージング法.

5. 第 22 回日本脳循環代謝学会総会 (大阪), 2010/11/26~27 (口演). 冨田裕, 安部貴人, 畝川美悠紀, 鳥海春樹, 正本和人, 菅野巌, 鈴木則宏. マウス中大脳動脈・永久閉塞モデルと虚血再灌流モデルとの *in vivo* 脳微小循環動態の比較.

(国際学会)

6. 9th World Congress for Microcirculation (Paris), 2010/10/25~28 (口演).Tomita Y., Abe T., Unekawa M., Toriumi H., Masamoto K., Kanno I., Suzuki N. Long-term *in vivo* investigation of mouse cerebral microcirculation after middle cerebral artery ischemia-reperfusion induced by the suture method.
7. 9th World Congress for Microcirculation (Paris), 2010/10/25~28 (ポスター).Toriumi H., Shimizu T., Shibata M., Tomita M., Tomita Y., Unekawa M., Kanno I., Suzuki N. Significance of arterio-venous shunt in the diploic veins in mice.
8. 9th World Congress for Microcirculation (Paris), 2010/10/25~28 (ポスター).Unekawa M., Tomita M., Tomita Y., Toriumi H., Kanno I., Suzuki N. Sustained decrease of red blood cell velocity in intraparenchymal capillaries against potassium-induced cortical spreading depression in rats.
9. 7th World Stroke Congress (Seoul), 2010/11/13~16 (ポスター).Tomita Y., Abe T., Unekawa M., Toriumi H., Masamoto K., Kanno I., Suzuki N. *In vivo* visualization of mouse cerebral microcirculation during middle cerebral artery occlusion induced by the suture method.

## G. 知的財産権の出願・登録状況

新規出願なし

別添５

表　研究成果の刊行に関する一覧表

| 刊行書籍又は雑誌名（雑誌のときは雑誌名、巻号数、論文名） | 刊行年月日 | 刊行書店名 | 執筆者名 |
|---|---|---|---|
| Response time of different methods of cardiac output monitoring during cardiopulmonary resuscitation and recovery. Journal of Cardiothoracic and Vascular Anesthesia. 24 (2): 306-308. | 2010 年 4 月 | Elsevier | Chimei Nishiwaki, Yoshifumi Kotake, Takeshige Yamada, Hiromasa Nagata, Manabu Tagawa, Junzo Takeda |
| Remifentanil for awake thoracoscopic bullectomy. J Cardiothorac Vasc Anesth 24(2): 386-387. | 2010 年 4 月 | | Kei Inoue, Kiyoshi Moriyama, Junzo Takeda |
| Effect of toll-like receptor 4 inhibitor on LPS-induced lung injury. Inflamm Res. 59(10): 837-845. | 2010 年 4 月 | Springer Basel | Hiroyuki Seki, Sadatomo Tasaka, Koichi Fukunaga, Yoshiki Shiraishi, Kiyoshi Moriyama, Keisuke Miyamoto, Yasushi Nakano, Naoko Matsunaga, Katsunori Takashima, Tatsumi Matsumoto, Masayuki Ii, Akitoshi Ishizaka, Junzo Takeda |
| ベクロニウムとスキサメトニウムは捨てがたい。日臨麻会誌 30(3)：438-445. | 2010 年 5 月 | | 武田純三 |
| Dynein-and activity-dependent retrograde transport of autophagosomes in neuronal axons. Autophagy. 6(3): 378-385. | 2010 年 4 月 | | Kiyoshi Katsumata, Jun Nishiyama, Takafumi Inoue, Noboru Mizushima, Junzo Takeda, Michisuke Yuzaki |
| Regional spinal cord cooling using a countercurrent closed-lumen epidural catheter. Ann Thorac Surg 89: 1312-3. | 2010 年 6 月 | Elsevier | Hideyuki Shimizu, Atsuo Mori, Tatsuya Yamada, Akiko Ishikawa, Hideyuki Okano, Junzo Takeda, Ryohei Yozu |
| 気管切開が施行不能であった頸部海綿状血管腫の 1 病例。麻酔 59(5): 618-621. | 2010 年 5 月 | | 壽原 朋宏、森山 潔、細川 幸希、藍 公明、武田 純三 |

| | | | |
|---|---|---|---|
| Laudanosine has no effects on respiratory activity but induces non-respiratory excitement activity in isolated brainstem-spinal cord preparation of neonatal rats. Advances in Experimental Medicine and Biology. 669: 177-180. | 2010 年 | Springer Science + Business Media | Shigeki Sakuraba, Yuki Hosokawa, Yuki Kaku, Junzo Takeda, Shun-ichi Kuwana |
| Effect of JM-1232(-), a new sedative on central respiratory activity in newborn rats. Advances in Experimental Medicine and Biology. 669: 115-118. | 2010 年 | Springer Science + Business Media | Junya Kuribayashi, Shun-ichi Kuwana, Yuki Hosokawa, Eiki Hatori, Junzo Takeda |
| Thyroid transcription factor-1 influences the early phase of compensatory lung growth in adult mice. American Journal of Respiratory and Critical Care Medicine 181: 1397-1406. | 2010 年 2 月 | | Yusuke Takahashi, Yotaro Izumi, Mitsutomo Kohno, Tokuhiro Kimura, Masafumi Kawamura, Yasunori Okada, Hiroaki Nomori, Eiji Ikeda |
| A non-invasive thynoma that occured 29 years after complete resection of a non-invasive thymoma accompanied by a microthymoma. Japanese Journal of Clinical Oncology. 40(10): 986-988. | 2010 年 5 月 | Oxford University Press | Yoshikane Yamauchi, Mitsutomo Kohno, Tai Hato, Yuichiro Hayashi, Yotaro Izumi, Hiroaki Nomori |
| Mediastinal germ cell tumor with somatic-type malignancy: report of 5 stage I/II cases. Ann Thorac Surg 90: 1014-6. | 2010 年 3 月 | Elsevier | Keisuke Asakura, Yotaro Izumi, Tatsuhiko Ikeda, Yoshishige Kimura, Hirohisa Horinouchi, Yuichiro Hayashi, Hiroaki Nomori |
| Airway administration of dexamethasone, 3'-5'-cyclic adenosine monophosphate, and isobutyllmethylxanthine facilitates compensatory lung growth in adult mice. AJP-Lung Cell Mol Physiol 300: L453-L461. | 2011 年 3 月 | American Physiological Society | Yusuke Takahashi, Yotaro Izumi, Mitsutomo Kohno, Masafumi Kawamura, Eiji Ikeda, Hiroaki Nomori |
| On freeze-thaw sequence of vital organ of assuming the cryoablation for malignant lung tumors by using cryoprobe as heat source. Cryobiology. 61: 317-326. | 2010 年 10 月 | Elsevier | Seishi Nakatsuka, Hideki Yashiro, Masanori Inoue, Sachio Kuribayashi, Masafumi Kawamura, Yotaro Izumi, Norimasa Tsukada, Yoshikane Yamauchi, Kohei Hashimoto, Kansei |

| | | | |
|---|---|---|---|
| | | | Kwata, Taisuke Nagasawa, Yi-Shan Lin |
| Effect of cutting technique at the intersegmental plane during segmentectomy on expansion of the preserved segment: comparison between staplers and scissors in ex vivo pig lung. European Journal of Cardio-Thoracic Surgery. | 印刷中 | Elsvier | Keisuke Asakura, Yotaro Izumi, Mitsutomo Kohno, Takashi Ohtsuka, Masayuki Okui, Kohei Hashimoto, Takashi Nakayama, Hiroaki Nomori |
| Superior plasma retention of a cross-linked human serum albumin dimmer in nephrotic rats as a new type of plasma expander. Drug Metabolism and Disposition. 38 (12): 2124-2129. | 2019 年 9 月 | American Society for Pharmacology and Experimental Therapeutics | Kazuaki Taguchi, Yukino Urata, Makoto Anraku, Hiroshi Watanabe, Keiichi Kawai, Teruyuki Komatsu, Eishun Tsuchida, Toru Maruyama, Masaki Otagiri |
| Virus trap in human serum albumin nanotube. Journal of the American Chemical Society. 133: 3246-3248. | 2011 年 2 月 | | Teruyuki Komatsu, Xue Qu, Hiromi Ihara, Mitsuhiro Fujiwara, Hiroshi Azuma, Hisami Ikeda |
| Protein nanotubes bearing a magnetite surface exterior. Polymers Advanced Technologies. 1-4. | 2010 年 12 月 | John Wiley & Sons | Teruyuki Komatsu, Nao Kobayashi |
| RBC velocities in single capillaries of mouse and rat brains are the same, despite 10-fold difference in body size. Brain Research 1320: 69-73. | 2010 年 2 月 | Elsevier | Miyuki Unekawa, Minoru Tomita, Yutaka Tomita, Haruki Toriumi, Koichi Miyaki, Norihiro Suzuki |
| Association of a cyclin-dependent kinase 5 regulatory subunit-associated protein 1-like (CDKAL1) polymorphism with elevated hemoglobin $A_{1c}$ levels and the prevalence of metabolic syndrome in Japanese men: interaction with dietary energy intake. American Journal of Epidemiology. 172 (9): 985-991. | 2010 年 9 月 | Oxford University Press | Koichi Miyaki, Than Oo, Yixuan Song, Htay Lwin, Yutaka Tomita, Haruhiko Hoshino, Norihiro Suzuki, Masaaki Muramatsu |
| Long term, repeated measurements of mouse cortical microflow at the same region of interest with high spatial | 2010 年 11 月 | Elsevier | Yutaka Tomita, Elisabeth Pinard, Alexy Tran-Dinh, Istvan Schiszler, Nathalie |

| | | | |
|---|---|---|---|
| resolution.<br>Brain Research. 1372: 59-69. | | | Kubis, Minoru Tomita, Norihiro Suzuki, Jacques Seylaz |
| Developmental and circulatory profile of the diploic veins.<br>Microvascular Research 81: 97-102. | 2010 年 11 月 | Elsevier | Haruki Toriumi, Toshihiko Shimizu, Mamoru Shibata, Miyuki Unekawa, Yutaka Tomita, Minoru Tomita, Norihiro Suzuki |
| Oscillating neuro-capillary coupling during cortical spreading depression as observed by tracking of FITC-labeled RBCs in single capillaries.<br>Neuroimage. | 印刷中 | Elsevier | Minoru Tomita, Yutaka Tomita, Miyuki Unekawa, Haruki Toriumi, Norihiro Suzuki |

# 研究成果の刊行物・別冊

(2010.4～2011.3)

# Response Time of Different Methods of Cardiac Output Monitoring During Cardiopulmonary Resuscitation and Recovery

Chiemi Nishiwaki, MD,* Yoshifumi Kotake, MD, PhD,† Takashige Yamada, MD,* Hiromasa Nagata, MD,* Manabu Tagawa, MD,‡ and Junzo Takeda, MD, PhD*

THE MOST COMMONLY used method of cardiac output (CO) monitoring during anesthesia and intensive care is continuous thermodilution with a pulmonary artery catheter (PAC), although several concerns have been raised about its usage because of the lack of a clear clinical advantage. Recently, less invasive CO monitoring devices have been introduced for clinical use. Although comparisons between these new devices and the traditional continuous thermodilution method have been reported in the literature, the performance of these monitors during profound hemodynamic changes or during critical events has rarely been reported. The authors experienced an unexpected case of intraoperative coronary artery spasm that required closed-chest compression. The authors coincidently monitored CO by esophageal Doppler, partial $CO_2$ rebreathing, and a PAC. How these monitors performed during cardiopulmonary resuscitation (CPR) and after the restoration of spontaneous circulation is reported.

## CASE REPORT

A 58-year-old man with an infrarenal aortic aneurysm was admitted for elective aortic reconstruction surgery. Although the patient had no subjective symptoms such as chest pain or arrhythmia, and no history of hypertension, a preoperative echocardiographic evaluation revealed anteroseptal hypokinesis. However, a subsequent coronary angiographic evaluation showed no coronary artery stenosis, and all other preoperative laboratory data were within normal limits. Anesthesia was induced with intravenous fentanyl, propofol, and vecuronium and was subsequently maintained with sevoflurane in an oxygen–nitrous oxide mixture. An intra-arterial catheter was inserted into the patient's right brachial artery, and his arterial pressure was monitored continuously. Because the patient gave his consent to participate in a prospective study that evaluated the precision of several CO monitoring devices, CO was monitored continuously by using different modes: the esophageal Doppler (EDM; Cardio-Q, Deltex, UK), the partial $CO_2$ rebreathing device (NICO, ver. 4.2; Respironics-Novametrix, Wallingford, CT), and continuous thermodilution using a PAC. The EDM monitor used an average of 6 cardiac cycles, whereas the NICO monitor calculated CO every 3 minutes. Continuous thermodilution CO monitors incorporate 2 modes of calculation (ie, STAT CCO and trend CCO [Vigilance; Edwards Lifesciences, Irvine, CA]). The measured data from these monitors were downloaded to a personal computer for further examination. Before incision, the patient's CO was measured as 3.4 L/min, 3.8 L/min, 3.6 L/min, and 3.6 L/min via the EDM, NICO, STAT CCO, and trend CCO monitors, respectively. End-tidal $CO_2$ partial pressure ($PETCO_2$) and mixed venous hemoglobin oxygen saturation ($SvO_2$) also were continuously monitored and recorded.

During the laparotomy, hypotension and tachycardia were noted and were accompanied by facial flushing. This was diagnosed as mesenteric traction syndrome and was treated with fluid administration and intermittent intravenous ephedrine. During this period, high cardiac output was recorded with all devices. The maximal values recorded were 6.9 L/min, 9.2 L/min, 17.4 L/min, and 17.9 L/min via the EDM, NICO, STAT CCO, and trend CCO monitors, respectively. At this point, the $SvO_2$ was 89% and $VCO_2$ was 137 mL/min. These symptoms eventually disappeared, and the patient's CO subsequently stabilized (measured as 5.5 L/min, 5.1 L/min, 10.1 L/min, and 11.3 L/min via the EDM, NICO, STAT CCO, and CCO monitors, respectively; $SvO_2$ 85%, $VCO_2$ 126 mL/min. The CO at this point as measured with a bolus thermodilution was 7.0 L/min.

During surgical exposure of the aortic aneurysm, a sudden onset of ventricular premature contraction was followed by sustained ventricular tachycardia (VT). Because initial DC cardioversion failed to stop the VT, phenylephrine, lidocaine, nitroglycerin, and epinephrine were administered while closed-chest compression was provided. During CPR, the patient was manually ventilated to ensure adequate ventilation. The minute volume provided during CPR was between 11 L/min and 12 L/min. The third DC cardioversion finally restored the patient to sinus rhythm. The duration of VT was 9 minutes, and chest compression provided a systolic pressure of more than 60 mmHg and diastolic pressure of more than 20 mmHg during CPR.

The trend for the EDM, NICO, STAT CCO, and trend CCO monitors are summarized in Figure 1, along with $PETCO_2$ and $SvO_2$ during the CPR period. The CO measured with EDM varied from 0 to 2.5 L/min, and the signal of descending aortic blood flow caused by chest compression was clearly visible during this event using EDM. Three rebreathing cycles were used with a NICO monitor during CPR. The first rebreathing cycles were applied at 2 minutes after the onset of VT and the CO and $VCO_2$ were reported as 2.9 L/min and 104 mL/min, respectively. The second cycle was applied 5 minutes after the onset of VT and failed to estimate the CO. The third rebreathing cycle was applied at 8 minutes after the onset of VT, and the CO and $VCO_2$ were reported as 0.1 L/min and 175 mL/min, respectively. After the restoration of sinus rhythm, the patient's CO as measured by EDM was 2.0 to 2.9 L/min, and the CO as estimated by the NICO monitor 90 seconds after VT termination was 3.9 L/min. $VCO_2$ was between 130 and 160 mL/min during this period. STAT CCO slightly decreased after the onset of VT but remained high for 6 minutes. Thereafter, it significantly decreased to 3.6 L/min and significantly increased 4 minutes after the return of spontaneous circulation. The trend CCO slightly decreased after the onset of VT but remained high during and after VT. In contrast, the $SvO_2$ promptly decreased after the onset of VT and returned to the pre-event value after the restoration of sinus rhythm.

The esophageal probe of the EDM was replaced with the probe for transesophageal echocardiography (TEE) for diagnosis and hemodynamic assessment. A subsequent electrocardiogram showed significant ST elevation in the anterior chest lead, and TEE indicated severe regional wall motion abnormalities. As such, the surgery was postponed. Hemodynamic stability was achieved with low-dose dopamine and a nitroglycerin infusion, and regional wall motion abnormalities were not detected at this point. These findings, as well as a negative preoperative coronary angiographic study, revealed coronary artery spasm as the cause of the VT. The patient was successfully extubated after surgery without any neurologic or cardiac sequelae. He was

*From the *Department of Anesthesiology, Keio University School of Medicine; †Department of Anesthesiology, Toho University; and ‡Department of Anesthesiology, Hakodate Municipal Hospital, Tokyo, Japan.*

*Address reprint requests to Yoshifumi Kotake, MD, Department of Anesthesiology, Toho University, 6-11-1, Ohmori Nishi, Ohta, Tokyo 143-8541, Japan. E-mail: ykotake@med.toho-u.ac.jp*



*1053-0770/10/2402-0016$36.00/0*

*doi:10.1053/j.jvca.2009.03.024*

*Key words: vascular anesthesia, monitoring, cardiovascular system, resuscitation*

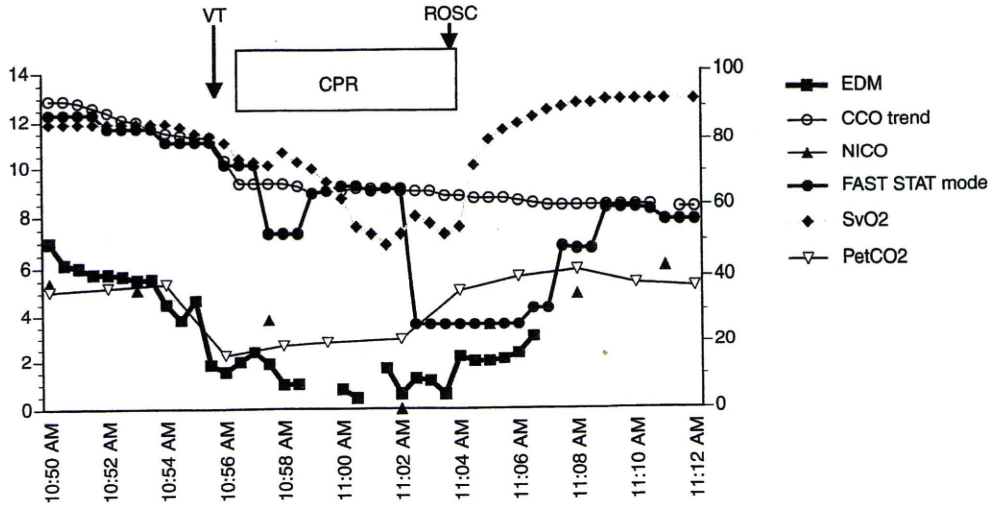


**Fig 1. Trends of the esophageal Doppler monitor (closed square, EDM, Cardio-Q, Deltex), NICO (closed triangle, Novametrix-Respironics), trend continuous thermodilution (trend CCO, open circle, Vigilance, Edwards Lifescience), STAT continuous thermodilution (STAT CCO, closed circle, Vigilance, Edwards Lifesciences), end-tidal $PCO_2$ ($PETCO_2$, Novametrix-Respironics), and mixed venous hemoglobin oxygen saturation ($SvO_2$, diamond, Vigilance, Edwards Life Science) were plotted. The left y-axis represents the EDM, NICO, trend CCO, and STAT CCO values, whereas the right y-axis represents the $PETCO_2$ and $SvO_2$. Data for CCO, STAT CCO, and $SvO_2$ were downloaded every 30 seconds. The averaged data of EDM for every 30 seconds were used to construct this graph. NICO estimated cardiac output every 3 minutes. Epochs with insufficient data were eliminated from the plot. The onset of VT, return of spontaneous circulation (ROSC), and the duration of CPR also are shown in this graph.**

discharged from the hospital without any complications and was scheduled for endovascular stenting at a later date.

## DISCUSSION

In this report, 3 devices using different systems for CO monitoring, EDM, NICO, and CCO monitors showed various trends of cardiac output during successful CPR. The data presented here provide important information about CO, blood flow distribution during CPR, and the response time of these CO monitors.

Before the onset of VT, the CO derived from continuous thermodilution showed much higher values than that derived from the other methods, including conventional bolus thermodilution. The authors believe that the true CO value was probably between the EDM, NICO, and CCO values because EDM and NICO tend to underestimate CO, whereas CCO tends to overestimate it. The abrupt increases of STAT CCO as well as trend CCO coincided with the hypotensive episode, possibly triggered by mesenteric traction. Significant vasodilation and medical intervention with vasoactive agents and the rapid infusion of fluid may have contributed to the large discrepancy.

There are only a limited number of studies regarding CO during CPR. Tucker et al[1] reported a stroke volume of 17.6 ± 5.2 mL measured by TEE during standard CPR. Redberg et al[2] also reported similar results. Laboratory studies documented that the stroke volume was 32 ± 16 mL or 0.45 mL/kg during CPR in a 45- to 50-kg swine.[3,4] These data basically agree with the aforementioned clinical results, and the authors assume that the stroke volume generated with standard chest compressions is in the range of 15 to 30 mL in human beings. Thus, a CO in the 1.5 to 3 L/min range could be maintained during successful closed-chest compression when the frequency is 100/min.

Based on these assumptions, EDM provided a reasonable estimate of CO during CPR.[5] This finding supports the notion that EDM is a real-time hemodynamic monitor and is able to respond to profound hemodynamic changes in a real-time manner.[6] However, the CO measured by EDM during CPR was lower than the values previously reported during successful CPR. Because the Doppler signal of descending aortic blood flow was clearly distinguishable even during the chest compression, the authors suggest chest compression may not significantly disturb the measurement of descending aortic blood flow by Doppler. Rather, the discrepancy can be explained partially explained by the different CO distribution during CPR. EDM actually measures descending aortic blood flow and assumes that 70% of the stroke volume distributes to the lower body via the descending aorta. Some studies have pointed out that blood flow to the lower body was significantly reduced, whereas the blood flow to the brain and myocardium were relatively preserved.[7,8] Despite this limitation, the authors' experience suggests that EDM may be very useful to ensure optimal chest compressions because the effectiveness of chest compressions can be evaluated directly by examining the aortic blood flow. It is evident that TEE offers a wider array of diagnostic information to guide therapy than EDM. However, the authors believe that EDM is more easily applicable to monitor the adequacy of chest compression during CPR because TEE is more operator-dependent and requires expertise for correct assessment.

It is not surprising that the NICO monitor was unable to provide realistic estimates of CO during the entire CPR process because this monitor uses a relatively complicated assumption and is dependent on stable $CO_2$ elimination via the lungs. However, the NICO monitor provided reasonable estimates of

CO during the early part of CPR and also after successful resuscitation. The $PETCO_2$ correlated well with the cardiovascular conditions. This case was also characterized by high $SvO_2$ values during the episode. The signal quality of $SvO_2$ transiently decreased at the onset of the episode, but otherwise it was good.

Both STAT CCO and trend CCO showed a small decline at the onset of VT, but remained more than 8 L/min during the majority of the CPR process. It is unlikely that such a high CO was maintained during CPR, and the authors believe that the overestimation of CO just before the onset of VT and the slow response time of the CCO were responsible for this apparent discrepancy. This speculation is supported by several previous reports that CCO may lag 5 to 15 minutes behind the true CO.[9-11] In contrast, $SvO_2$ rapidly decreased during the episode of VT and quickly returned to normal after successful defibrillation. This finding supports the notion that $SvO_2$ provides more crucial information than CCO in critical situations involving hemodynamic instability.[12]

The STAT CCO followed the hemodynamic change with a 6-minute delay after the onset of VT and a 4-minute delay after recovery. The trend CCO showed a more prolonged delay, and 9 minutes of low flow during CPR were completely undetected. The authors' experience agrees with the previous report that significant alterations in CO after pacing-induced hemodynamic changes were detected within 90 seconds via $SvO_2$ and within 270 seconds via STAT CCO, whereas trend CCO failed to increase within 6 minutes.[13] Therefore, with CCO the STAT mode should be used to assess the CO during rapid hemodynamic changes.

In conclusion, EDM provided real-time monitoring of CO during sustained ventricular tachycardia and may provide important information about the adequacy of resuscitation measures. Although NICO only estimates CO intermittently, it successfully calculated CO within 2 minutes after successful resuscitation. In contrast, STAT CCO showed a significant delay, and trend CCO showed an even longer delay. Furthermore, the trend CCO was unable to detect the clinical condition, which is necessary during chest compressions. This case report shows the possible usefulness of EDM during CPR and provides some information about the response time of various CO monitors during profound hemodynamic changes.

## REFERENCES


1. Tucker KJ, Redberg RF, Schiller NB, et al: Active compression-decompression resuscitation: Analysis of transmitral flow and left ventricular volume by transesophageal echocardiography in humans. Cardiopulmonary Resuscitation Working Group. J Am Coll Cardiol 22:1485-1493, 1993

2. Redberg RF, Tucker KJ, Cohen TJ, et al: Physiology of blood flow during cardiopulmonary resuscitation. A transesophageal echocardiographic study. Circulation 88:534-542, 1993

3. Klouche K, Weil MH, Sun S, et al: Stroke volumes generated by precordial compression during cardiac resuscitation. Crit Care Med 30:2626-2631, 2002

4. Pernat A, Weil MH, Sun S, et al: Stroke volumes and end-tidal carbon dioxide generated by precordial compression during ventricular fibrillation. Crit Care Med 31:1819-1823, 2003

5. Lichtenberger M, DeBehnke D, Crowe DT, et al: Comparison of esophageal Doppler monitor generated minute distance and cardiac output in a porcine model of ventricular fibrillation. Resuscitation 41:269-276, 1999

6. Marik PE: Pulmonary artery catheterization and esophageal Doppler monitoring in the ICU. Chest 116:1085-1091, 1999

7. Taylor RB, Brown CG, Bridges T, et al: A model for regional blood flow measurements during cardiopulmonary resuscitation in a swine model. Resuscitation 16:107-118, 1988

8. Duggal C, Weil MH, Gazmuri RJ, et al: Regional blood flow during closed-chest cardiac resuscitation in rats. J Appl Physiol 74:147-152, 1993

9. Haller M, Zollner C, Briegel J, et al: Evaluation of a new continuous thermodilution cardiac output monitor in critically ill patients: A prospective criterion standard study. Crit Care Med 23:860-866, 1995

10. Siegel LC, Hennessy MM, Pearl RG: Delayed time response of the continuous cardiac output pulmonary artery catheter. Anesth Analg 83:1173-1177, 1996

11. Aranda M, Mihm FG, Garrett S, et al: Continuous cardiac output catheters: Delay in in vitro response time after controlled flow changes. Anesthesiology 89:1592-1595, 1998

12. Nelson LD: The new pulmonary artery catheters: continuous venous oximetry, right ventricular ejection fraction, and continuous cardiac output. New Horiz 5:251-258, 1997

13. Lazor MA, Pierce ET, Stanley GD, et al: Evaluation of the accuracy and response time of STAT-mode continuous cardiac output. J Cardiothorac Vasc Anesth 11:432-436, 1997

42°C, easily resulting in perfusate temperatures exceeding 37°C, which could be delivering hyperthermic perfusate to the brain and yet not be reflected in NP temperatures that are not allowed to exceed 37°C.

The concern is that the patients in the first group who were rewarmed to NP temperatures of 37°C may, in fact, have been transiently exposed to cerebral temperatures of 40° or 41°C from the perfusate using the gradients they described. This could have contributed to the statistically significant deterioration in neurocognitive function observed in their 37°C group of patients when compared with those patients warmed only to 33°C. The key message is that the perfusionist should always monitor perfusate temperatures not only to maintain appropriate gradients between the patient's core temperature and the perfusate when rewarming (and cooling) but also not to allow the perfusate to exceed 37.5°C to 38°C as the NP temperature approaches 37°C.

*Mark Kurusz, LP, CCP*
Capital Area Perfusionists, Inc
Austin, TX

REFERENCE

1. Sahu B, Chauhan S, Kiran U, et al: Neurocognitive function in patients undergoing coronary artery bypass graft surgery with cardiopulmonary bypass: The effect of two different rewarming strategies. J Cardiothorac Vasc Anesth 23:14-21, 2009

doi:10.1053/j.jvca.2009.06.016

## Remifentanil for Awake Thoracoscopic Bullectomy

*To the Editor:*

We report a case of video-assisted thoracoscopic surgery (VATS) performed under epidural anesthesia in a patient with acute respiratory failure. In this patient, remifentanil was infused alone not to sedate the patient but to slow his respiratory rate while keeping him awake.

A 61-year-old man was brought to the emergency room complaining of left-sided chest pain. This patient had been on home oxygenation and steroid therapy for cystic fibrosis since he was 60 years old and was diagnosed as having left-sided lung cancer. After chemotherapy was initiated, he suffered from lung infection with the subsequent development of acute respiratory failure. When an increased dose of steroid was initiated, he suddenly had left-sided chest pain and dyspnea. A computed tomography scan showed multiple bilateral bullae. Although 2 chest tubes were inserted for 3 days, there was massive persistent air leakage, and his arterial oxygen tension was 86.2 mmHg under 70% of oxygen inspiration. Because the left lung did not completely expand, video-assisted thoracoscopic bullectomy was scheduled.

Because the patient had multiple bilateral bullae, we planned video-assisted thoracoscopic bullectomy under epidural anesthesia. An epidural catheter was placed at the Th 4/5 level and 30 mL of 0.5% ropivacaine were injected into the epidural space to achieve somatosensory and motor block at the T1 to T8 level while preserving diaphragmatic respiration. The surgical procedure was performed with the patient in the supine position. Because the patient had tachypnea (respiratory rate 32/min) caused by respiratory failure, the surgeon requested to decrease the respiratory rate for safety during the surgical procedure. Confirming that the patient did not have hypercapnea ($PaCO_2$: 42 mmHg), a continuous infusion of remifentanil was initiated to slow the respiratory rate while keeping the patient awake.

The patient's respiratory rate gradually decreased from 30/min to 15/min by increasing the dose of remifentanil from 0.005 μg/kg/min up to 0.06 μg/kg/min. A continuous infusion of phenylephrine was initiated as blood pressure gradually decreased by increasing the dose of remifentanil. Even at 0.06 μg/kg/min of remifentanil infusion, the patient was still awake and able to take deep breaths or speak loudly, whereas the respiratory rate decreased to 15/min and $PaCO_2$ reached 52.8 mmHg (pH = 7.382, $PaO_2$ = 106.7 mmHg). At the time of bulla resection, the surgeon requested apnea for a moment. After 100% oxygen inhalation, a bolus dose of 10 μg of remifentanil was injected and the respiratory rate decreased to 6/min, whereas $PaCO_2$ reached 70.6 mmHg (pH = 7.309, $PaO_2$ = 185.5 mmHg). The bulla was safely resected, and the respiratory rate returned to 15/min within 1 minute after the remifentanil bolus.

Traditionally, VATS is performed under general anesthesia, with the use of double-lumen endobronchial intubation and single-lung ventilation. To avoid the risks of general anesthesia with one-lung ventilation, VATS under local or epidural anesthesia has been performed in high-risk patients[1-3] and has been shown to provide faster postoperative recovery for minimally invasive thoracoscopic surgery. Pompeo and Mineo[4] combined thoracic epidural anesthesia with a continuous propofol infusion for awake pulmonary metastasectomy. In addition to sedative drugs, opioids have been successfully added for analgesia and sedation. Gravino et al[5] reported that monitored anesthesia care using midazolam and a continuous infusion of both sufentanil and remifentanil gave satisfactory analgesia and sedation for video-assisted talc pleurodesis.[5]

In this case, in addition to thoracic epidural anesthesia, we used remifentanil, a titratable opioid with quick onset and washout, in order to slow the respiratory rate during bulla resection. The patient was kept awake during the procedure. As expected, the continuous infusion of remifentanil gradually slowed the respiratory rate in a dose-dependent manner. In addition, a bolus dose of 10 μg of remifentanil safely decreased the respiratory rate to 6/min, with quick recovery to 15/min within 1 minute. The decreased respiratory rate was accompanied by the development of hypercapnia, which was of little physiologic consequence in the presence of generous supplemental oxygen.

*Kei Inoue, MD**
*Kiyoshi Moriyama, MD†*
*Junzo Takeda, MD**
*Department of Anesthesiology
Keio University School of Medicine
Tokyo, Japan
†Department of Anesthesiology
Kyorin University School of Medicine
Tokyo, Japan

## REFERENCES

1. Mineo TC: Epidural anesthesia in awake thoracic surgery. Eur J Cardiothorac Surg 32:13-19, 2007

2. Mukaida T, Andou A, Date H, et al: Thoracoscopic operation for secondary pneumothorax under local and epidural anesthesia in high-risk patients. Ann Thorac Surg 65:924-926, 1998

3. Nezu K, Kushibe K, Tojo T, et al: Thoracoscopic wedge resection of blebs under local anesthesia with sedation for treatment of a spontaneous pneumothorax. Chest 111:230-235, 1997

4. Pompeo E, Mineo TC: Awake pulmonary metastasectomy. J Thorac Cardiovasc Surg 133:960-966, 2007

5. Gravino E, Griffo S, Gentile M, et al: Comparison of two protocols of conscious analgosedation in video-assisted talc pleurodesis. Minerva Anestesiol 71:157-165, 2005

doi:10.1053/j.jvca.2009.05.012

Inflamm. Res.
DOI 10.1007/s00011-010-0195-3

Inflammation Research

ORIGINAL RESEARCH PAPER

# Effect of Toll-like receptor 4 inhibitor on LPS-induced lung injury

Hiroyuki Seki · Sadatomo Tasaka · Koichi Fukunaga · Yoshiki Shiraishi · Kiyoshi Moriyama · Keisuke Miyamoto · Yasushi Nakano · Naoko Matsunaga · Katsunori Takashima · Tatsumi Matsumoto · Masayuki Ii · Akitoshi Ishizaka · Junzo Takeda

Received: 2 September 2009 / Revised: 25 December 2009 / Accepted: 29 March 2010


## Abstract

*Objective and design* Toll-like receptor 4 (TLR4) plays important roles in the recognition of lipopolysaccharide (LPS) and the activation of inflammatory cascade. In this study, we evaluated the effect of TAK-242, a selective TLR4 signal transduction inhibitor, on acute lung injury (ALI).

*Materials and methods* C57BL/6J mice were intravenously treated with TAK-242 15 min before the intratracheal administration of LPS or Pam3CSK4, a synthetic lipopeptide. Six hours after the challenge, bronchoalveolar lavage fluid was obtained for a differential cell count and the measurement of cytokine and myeloperoxidase levels. Lung permeability and nuclear factor-κB (NF-κB) DNA binding activity were also evaluated.

*Results* TAK-242 effectively attenuated the neutrophil accumulation and activation in the lungs, the increase in lung permeability, production of inflammatory mediators, and NF-κB DNA-binding activity induced by the LPS challenge. In contrast, TAK-242 did not suppress inflammatory changes induced by Pam3CSK4.

*Conclusion* TAK-242 may be a promising therapeutic agent for ALI, especially injuries associated with pneumonia caused by Gram-negative bacteria.

**Keywords** Toll-like receptor 4 · Endotoxin · Acute lung injury · Rodent · NF-κB

Responsible Editor: K. Visvanathan.

H. Seki · K. Moriyama · J. Takeda
Department of Anesthesiology, Keio University School of Medicine, Tokyo, Japan

S. Tasaka (✉) · K. Fukunaga · Y. Shiraishi · K. Miyamoto · Y. Nakano · A. Ishizaka
Division of Pulmonary Medicine, Keio University School of Medicine, 35 Shinanomachi, Shinjuku-ku, Tokyo 160-8582, Japan
e-mail: tasaka@cpnet.med.keio.ac.jp

N. Matsunaga · K. Takashima · T. Matsumoto · M. Ii
Pharmaceutical Research Division, Takeda Pharmaceutical Co. Ltd., Osaka, Japan

Published online: 13 April 2010

## Introduction

Over the last few decades, several studies have indicated that the survival rate for patients with acute lung injury (ALI) or acute respiratory distress syndrome (ARDS) has improved, although the mortality rate remains high, ranging between 25 and 40% [1]. ALI/ARDS may occur in association with direct lung injury, including pneumonia, aspiration of gastric contents, and inhalation of noxious gas, or indirect lung injury, such as sepsis, blood transfusions and shock. Among the various predisposing factors, severe pneumonia is one of the most common causes [2]. Experimental endotoxin (lipopolysaccharide; LPS) administration via the tracheal route has been extensively used to study the pathogenesis of ALI/ARDS following severe pneumonia [3].

Toll-like receptors (TLRs) have been shown to play an essential role in the activation of innate immunity by recognizing specific patterns of microbial components [4]. Among the TLRs, TLR4 recognizes LPS, triggers the activation of an intracellular signaling pathway involving nuclear factor-κB (NF-κB), and results in the upregulation of adhesion molecules and inflammatory mediators, such as cytokines and chemokines. TLR4 mutant (C3H/HeJ) mice have been shown to be hyporesponsive to LPS [5] and do

not develop ALI after being challenged with aerosolized LPS [6]. Conversely, the overexpression of TLR4 in transgenic mice augmented the responses to inhaled LPS, including bronchoconstriction, the production of tumor necrosis factor (TNF) and keratinocyte-derived chemokine (KC), lung epithelial and endothelial cell damage, and the recruitment of neutrophils in the lung [7].

To date, many clinical trials have been conducted to examine the efficacy of blocking a single inflammatory mediator in patients with ALI/ARDS, but none of them have shown a sufficient efficacy for clinical application [8, 9]. Since these outcomes could be due to the combined contribution of various pathogenic mediators, we hypothesized that a treatment strategy aimed at inhibiting the upstream inflammatory signaling pathway, such as TLR4, might be reasonable. In fact, a synthetic lipid A analogue that functions as a TLR4 antagonist reportedly showed protective effects against septic shock in mice [10].

TAK-242, a selective TLR4 signal transduction inhibitor, has been shown to suppress LPS-induced inflammatory responses in vitro [11] and lethality after systemic LPS challenge in vivo [12]. In this study, we evaluated the effect of TAK-242 using a murine model of ALI induced by an intratracheal LPS challenge. We examined inflammatory cell recruitment; lung permeability; the levels of pro-inflammatory cytokines, chemokines, myeloperoxidase (MPO) in bronchoalveolar lavage (BAL) fluid; and NF-$\kappa$B DNA-binding activity. In addition, to elucidate whether the effect of TAK-242 is specifically through the inhibition of the TLR4 pathway, we evaluated the effect of TAK-242 treatment on the inflammatory cell accumulation and cytokine production in the lungs following an intratracheal challenge of Pam3CSK4, a potent activator of TLR2/TLR1 pathway.

## Materials and methods

### Materials

TAK-242, ethyl (6*R*)-6-[*N*-(2-chloro-4-fluorophenyl)sulfamoyl]cyclohex-1-ene-1-carboxylate (molecular weight; 362 Da), was synthesized at Takeda Pharmaceutical Company Limited (Osaka, Japan). TAK-242 was dissolved in a fat emulsion. Pam3CSK4, (*S*)-[2,3-Bis (palmitoyloxy)-(2-*RS*)-propyl]-*N*-palmitoyl-(*R*)-Cys-(*S*)-Ser-(*S*)-Lys4-OH·3HCl] was purchased from InvivoGen (San Diego, CA).

### Mice

Eight-week-old male C57BL/6J mice were obtained from Charles River Laboratories Japan (Yokohama, Japan). Mice were given free access to water and standard rodent chow and were housed in pathogen-free cages. All animal experiments were approved by the Animal Care and Use Committee of Keio University School of Medicine.

### Murine model of lung injury

Mice were anesthetized using intraperitoneal ketamine (50 mg/kg) and xylazine (5 mg/kg). During the following procedures, mice were spontaneously breathing. The trachea was exposed surgically and punctuated with a 24-gauge angiocatheter to instill 0.3 mg/kg of LPS from *Escherichia coli* O55:B5 (Sigma-Aldrich, St. Louis, MO) or phosphate-buffered saline (PBS) into the left lung. Fifteen minutes before the intratracheal administration of LPS, the animals received an intravenous injection of 0.3, 1.0, or 3.0 mg/kg of TAK-242 (LPS + TAK groups) or the vehicle alone (LPS control group) via the tail vein. The sham group animals received an intravenous injection of vehicle alone followed by the intratracheal administration of PBS.

In another series, mice were challenged intratracheally with 0.25 mg/kg of Pam3CSK4 15 min after an intravenous injection of 3.0 mg/kg of TAK-242 (Pam3 + TAK group) or the vehicle alone (Pam3 control group) via the tail vein.

### Bronchoalveolar lavage

Six hours after intratracheal instillation, the mice were euthanized with deep anesthesia using intraperitoneal pentobarbital sodium (50 mg/kg). The trachea was exposed and cannulated with a 20-gauge angiocatheter. Both lungs were lavaged with two separate 0.7-mL volumes of ice-cold PBS. The BAL fluid was centrifuged at $400\times g$ for 10 min at 4°C to pellet the cell fraction, and the supernatant was stored at −80°C until the measurements of the cytokines, chemokines, MPO, and human serum albumin (HSA) levels to calculate the permeability index. The cell pellet was resuspended in 400 μL of cold saline, and the total cell counts were determined using a hemacytometer. Differential cell counts were performed using cytocentrifuge smears stained with Diff-Quik (Sysmex, Kobe, Japan).

### Measurement of proinflammatory mediators in bronchoalveolar lavage fluid

BAL fluid was assayed for TNF-$\alpha$, interleukin (IL)-1$\beta$, IL-6, macrophage inflammatory protein (MIP)-2 and KC using a multiplex cytokine bead array system (Bio-Plex™; Bio-Rad, Hercules, CA) according to the manufacturer's instructions. The reaction mixture was read using the Bio-Plex protein array reader, and the data were analyzed using the Bio-Plex Manager software program. Interferon-

gamma inducible protein (IP)-10 (CXCL10) in BAL fluid was quantified using an ELISA kit (R&D Systems, Minneapolis, MN). MPO in the BAL fluid was assayed using an ELISA kit (Hycult Biotechnology, Uden, The Netherlands).

### Lung permeability index

Mice were given 10 mg/kg of HSA dissolved in 100 μL of saline intravenously, 1 h before euthanasia. At the time of sacrifice, the blood was drawn from the inferior vena cava. The permeability index was defined as the ratio of the HSA concentration in the BAL fluid to that in the plasma, presented as a percentage. The HSA concentration was measured using an immunoassay with a Human Albumin ELISA Quantitation Kit (Bethyl Laboratories, Montgomery, TX). The lower limit of detection was 5 ng/mL.

### NF-κB (p65) DNA-binding activity in the lung

#### *Nuclear protein extraction*

After performing BAL, the left lungs were harvested and snap frozen in liquid nitrogen and then stored at −80°C until analysis. The lungs were homogenized in 2 mL of ice-cold Buffer A (10 mM HEPES, 1.5 mM $MgCl_2$, 10 mM KCl, 0.5 mM DTT, 0.5 mM PMSF) with a 0.1% volume of Nonidet P-40 and a protease inhibitor cocktail (1 mg/mL leupeptin, 1 mg/mL aprotinin, 10 mg/mL soy bean trypsin inhibitor, 1 mg/mL pepstatin). Following 10 min of incubation on ice, the homogenates were centrifuged at 850×*g* for 10 min at 4°C. The pellets were resuspended in 2 mL of Buffer A and centrifuged at 1,200×*g* for 10 min at 4°C. The crude nuclear pellets were resuspended in 40 mL of Buffer B (20 mM HEPES, 1.5 mM $MgCl_2$, 0.42 M NaCl, 0.2 mM EDTA, 25% vol/vol glycerol, 0.5 mM DTT, 0.5 mM PMSF) with a protease inhibitor cocktail (as described above) and incubated for 30 min on ice. Nuclear extracts were recovered following centrifugation at 20,000×*g* for 15 min at 4°C and stored at −80°C. The protein concentration of the nuclear extracts was determined using a BCA Protein Assay Kit (Pierce, Rockford, IL) with bovine serum albumin used as a standard.

#### *NF-κB (p65) DNA-binding activity assay*

NF-κB (p65) DNA-binding activity was examined using the TransAM™ ELISA kit (Active Motif, Carlsbad, CA) according to the manufacturer's protocol. In brief, 0.5 μg of nuclear extract was subjected to the binding of NF-κB to an immobilized consensus sequence (5′-GGGACTTTC C-3′) in a 96-well plate, and the primary and secondary antibodies were added. After the colorimetric reaction, the samples were measured in a spectrophotometer at the wavelength of 450 nm. Recombinant NF-κB p65 (Active Motif) was used as a protein standard. The DNA binding specificity was assessed using wild-type or mutated oligonucleotides.

### Statistical analysis

Data are presented as the mean ± SEM. All statistical analyses were carried out using SAS software (version 6.1, SAS Institute, Cary, NC). Differences in the differential cell counts, permeability index and mediator levels in the BAL fluid in vehicle-treated versus TAK-242-treated groups were analyzed using a one-tailed Williams or one-tailed Shirley–Williams test. We chose these tests for analysis because Williams' test is more powerful than Dunnett's test for dose-related data [13, 14]. Differences between the sham and vehicle-treated groups were analyzed using a Student or Welch *t* test and were considered statistically significant when $P < 0.05$.

## Results

### Inhibitory effect of TAK-242 on inflammatory cell recruitment to the lung

Mice were treated with 0.3 mg/kg of LPS administered into the left lung; 6 h later, BAL fluid was obtained and used to perform a differential cell count. The total cell and neutrophil counts are shown in Fig. 1a, b. LPS instillation induced a significant increase in inflammatory cell recruitment into the alveolar space, compared with the instillation of PBS. Treatment with 3.0 mg/kg of TAK-242 effectively suppressed the total cell count in BAL fluid, compared with the control group ($P < 0.01$; Fig. 1a). It also markedly reduced the recruitment of neutrophils into the alveolar space ($P < 0.01$; Fig. 1b).

### Inhibitory effects of TAK-242 on cytokine, chemokine and MPO levels in BAL fluid

Six hours after LPS instillation, BAL fluid was recovered and the concentration of TNF-α, IL-1β, IL-6, KC, MIP2, IP-10, and MPO in the BAL fluid was measured. LPS instillation markedly increased the levels of these inflammatory cytokines and chemokines in the alveolar space (Fig. 2a–f). The MPO level in the BAL fluid was also significantly enhanced after LPS instillation, indicating neutrophil degranulation in the alveolar space (Fig. 2g). TAK-242 markedly inhibited the LPS-induced increase in TNF-α in a dose-dependent manner, compared with the

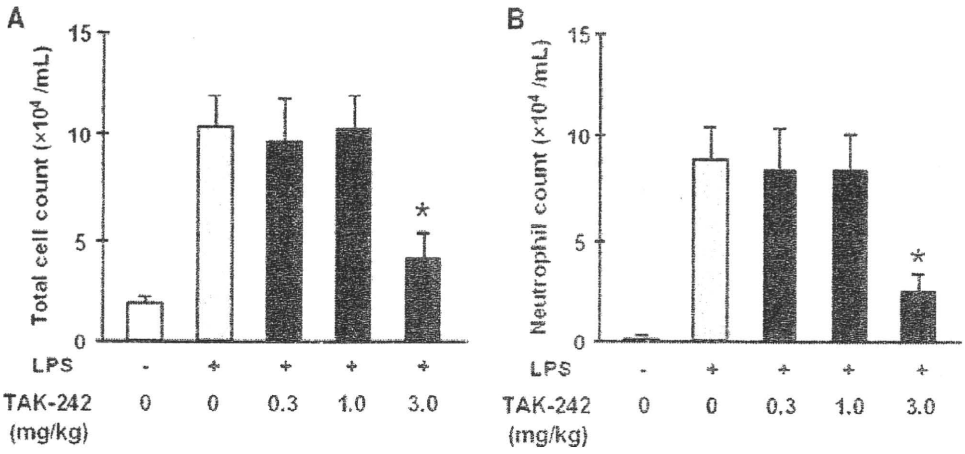


**Fig. 1** Inhibitory effect of TLR4 signaling blockade on inflammatory cell recruitment into the lung. Mice received an intravenous injection of 0.3, 1.0, or 3.0 mg/kg of TAK-242 (treatment groups, $n = 6$ for each group) or vehicle (control group, $n = 6$), followed by the administration of 0.3 mg/kg of LPS into the left lung; 6 h later, BAL fluid was obtained and used to perform a differential cell count. **a** TAK-242 (3.0 mg/kg) effectively suppressed the total cell number, compared with the control group. **b** TAK-242 (3.0 mg/kg) dramatically reduced the recruitment of neutrophils into the alveolar space. Values are the mean ± SD. $^*P < 0.025$ (one-tailed Williams test) compared with the control group (*gray bar*)

control group (Fig. 2a). Especially, 3.0 mg/kg of TAK-242 suppressed the elevation of TNF-$\alpha$ by 95%. Lower doses of TAK-242 (0.3 and 1.0 mg/kg) also suppressed the elevation in the TNF-$\alpha$ level by 55 and 80%, respectively, compared with the control group (Fig. 2a). In the mice treated with 3.0 mg/kg of TAK-242, the LPS-induced elevation of the IL-1$\beta$ level in the BAL fluid was reduced by 60% (Fig. 2b). Lower doses of TAK-242 also reduced the level of IL-1$\beta$ significantly (Fig. 2b). Treatment with 1.0 and 3.0 mg/kg of TAK-242 inhibited the elevation of IL-6 by 66 and 83%, respectively, compared with the control group (Fig. 2c). KC and MIP-2, murine homologs of the CXC chemokine family, are known to function as neutrophil chemoattractants and activators [15]. Treatment with 3.0 mg/kg of TAK-242 significantly inhibited the upregulation of KC and MIP-2 by 70 and 60%, respectively, compared with the control group (Fig. 2d, e). The level of IP-10, another CXC chemokine, was significantly decreased by TAK-242 treatment in a dose-dependent manner (Fig. 2f). Especially, 3.0 mg/kg of TAK-242 decreased the level of IP-10 to a level similar to that in the sham group. Treatment with 1.0 mg/kg of TAK-242 also inhibited the LPS-induced elevation of IP-10 by 85%, compared with the control group. A dose of 0.3 mg/kg of TAK-242 suppressed the upregulation of IP-10 by 50%, but the difference did not reach statistical significance. The administration of 3.0 mg/kg of TAK-242 markedly reduced the MPO level in the BAL fluid ($P < 0.01$), suggesting that TAK-242 might inhibit the degranulation of neutrophils (Fig. 2g). Although 0.3 and 1.0 mg/kg of TAK-242 suppressed the level of MPO in the BAL fluid by 30 and 50% respectively, compared with the control group, the difference did not reach statistical significance.

### Effect of TAK-242 on LPS-induced increase in lung permeability

The permeability index was calculated as the BAL fluid-to-plasma ratio of the concentration of human albumin that was injected intravenously 1 h before sacrifice. Thus, this index reflects pulmonary endothelial and alveolar septal permeability. The permeability index in the control group was significantly higher than that in the sham group ($0.048 \pm 0.011$ vs. $0.002 \pm 0.001\%$; $P < 0.01$), and treatment with TAK-242 (3.0 mg/kg) significantly suppressed the elevation of this index, compared with the control group ($0.015 \pm 0.005$ vs. $0.048 \pm 0.011\%$; $P < 0.01$) (Fig. 3). Although 1.0 mg/kg of TAK-242 decreased the permeability index by 40%, no significant differences in this index were seen between the control group and those treated with 0.3 or 1.0 mg/kg of TAK-242. We observed the exhibition of the animals carefully, but no difference was observed after the instillation.

### Inhibitory effect of TAK-242 on NF-$\kappa$B DNA-binding activity in the lung

To evaluate the effect of TAK-242 on the LPS-induced upregulation of the NF-$\kappa$B signaling pathway in the lung, nuclear extracts of lung homogenates were analyzed using the TransAM™ ELISA kit. Because the most frequently activated form of NF-$\kappa$B in TLR signaling is a heterodimer composed of Rel A(p65)-p50 [16] and p50 lacks the transcription activation domain, we used p65 as a marker of NF-$\kappa$B activation. As shown in Fig. 4, LPS stimulation induced high levels of NF-$\kappa$B DNA-binding activity. Treatment with 1.0 and 3.0 mg/kg of TAK-242 showed a

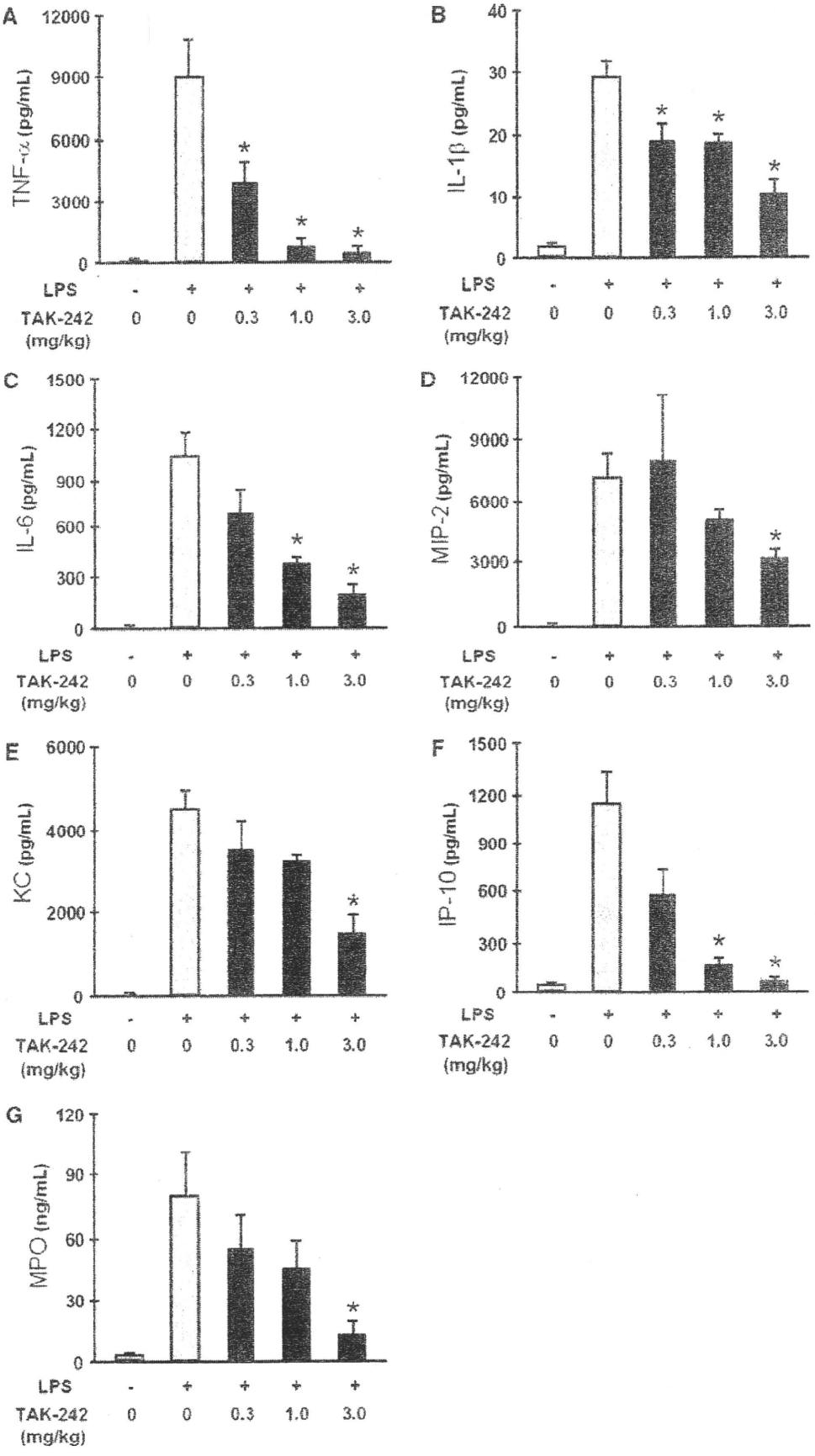


**Fig. 2** Inhibitory effect of TLR4 signaling blockade on cytokine, chemokine and MPO levels in BAL fluid. Six hours after LPS instillation. BAL fluid was recovered and the amounts of cytokines, chemokines and MPO were measured. **a** TAK-242 dramatically inhibited the LPS-induced increase in TNF-$\alpha$ in a dose-dependent manner, compared with the control group. **b** TAK-242 also reduced the level of IL-1$\beta$ significantly in a dose-dependent manner. **c** The elevation of IL-6 was effectively inhibited by treatment with 1.0 and 3.0 mg/kg of TAK-242. **d** TAK-242 (3.0 mg/kg) suppressed the level of MIP-2 significantly. **e** The level of KC was also suppressed by treatment with 3.0 mg/kg of TAK-242. **f** The level of IP-10 was strongly suppressed by treatment with TAK-242 in a dose-dependent manner. **g** Administration of TAK-242 markedly reduced the level of MPO in the BAL fluid. Values are the mean ± SD; $n = 6$ for each treatment group and vehicle. $^*P < 0.025$ (one-tailed Williams test) compared with the control group (*gray bar*)

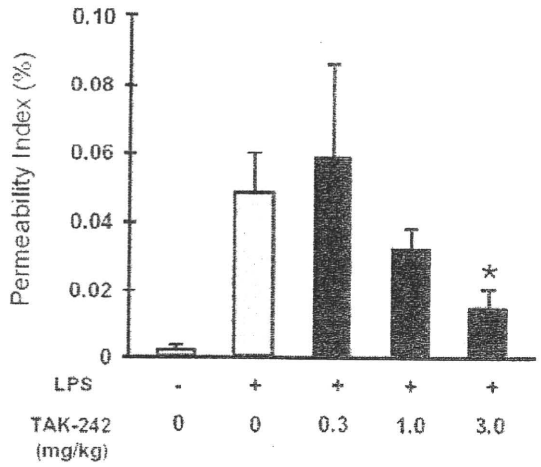


**Fig. 3** Effect of TLR4 signaling blockade on LPS-induced increase in lung permeability. The permeability index was calculated as the BAL fluid-to-plasma ratio of the concentration of human serum albumin injected intravenously 1 h before sacrifice. Treatment with 3.0 mg/kg of TAK-242 significantly suppressed the elevation of this index, compared with the control group. Values are the mean ± SD; $n = 6$ for each treatment group and vehicle. $^*P < 0.025$ (one-tailed Shirley–Williams test) compared with the control group (*gray bar*)

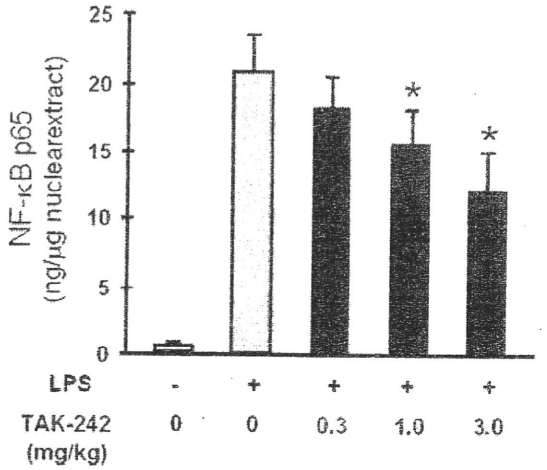


**Fig. 4** Inhibitory effect of TLR4 signaling blockade on NF-κB DNA-binding activity in the lung. To evaluate the effect of TAK-242 on the LPS-induced upregulation of the NF-κB signal pathway in the lung, nuclear extracts of lung homogenates were analyzed using the TransAM™ ELISA kit. TAK-242-treatment (1.0 and 3.0 mg/kg) produced a marked reduction in LPS-induced DNA–protein complex binding activity. Values are the mean ± SD; $n = 6$–7 for each treatment group and vehicle. $^*P < 0.025$ (one-tailed Williams test) compared with the control group (*gray bar*)

marked reduction in LPS-induced DNA–protein complex binding activity (Fig. 4). A lower dose (0.3 mg/kg) of TAK-242 did not significantly change the NF-κB DNA-binding activity. Additionally, the binding was specific, since the wild-type consensus oligonucleotide prevented NF-κB binding to the probe immobilized on the plate; conversely, the mutated oligonucleotide had no effects on NF-κB binding (data not shown).

### Effects of TAK-242 in Pam3CSK4-induced lung inflammation

To elucidate whether the effect of TAK-242 is specifically through the inhibition of TLR4 pathway, we evaluated the effect of TAK-242 on the inflammatory cell accumulation and cytokine production in the lungs following an intratracheal challenge of Pam3CSK4, a potent activator of TLR2/TLR1 pathway. Pam3CSK4 induced marked infiltration of inflammatory cells into the alveolar space (Fig. 5a, b) as well as inflammatory mediator production including IL-1β, IL-6 and KC (Fig. 6a–c). Treatment with TAK-242 did not inhibit the infiltration of inflammatory cells and the release of inflammatory mediators into the alveolar space elicited by Pam3CSK4.

## Discussion

In this study, we demonstrated that TAK-242 inhibited LPS-induced neutrophil recruitment and activation in the lung and lessened the LPS-induced increase in lung permeability. In addition, it attenuated the release of pro-inflammatory mediators into the alveolar space and inhibited the activation of the NF-κB signaling pathway. These results suggest that TAK-242, a specific inhibitor of TLR4 signaling, might be effective for the alleviation of LPS-induced lung injury. To the best of our knowledge, this is the first report on the effect of a synthesized TLR4 signaling inhibitor with a small molecular size on the production of inflammatory mediators and tissue injury after a locally administered inflammatory stimulus.

TLR4 has been shown to play a critical role in LPS recognition and subsequent signal transduction [17]. The activation of signaling requires CD14-bound LPS to adhere to and to transactivate the TLR4-myeloid differentiation protein (MD)-2 complex on the cell membrane [18–20]. TLR4 recruits four adaptor proteins, including myeloid differentiation factor 88 (MyD88), Toll/IL-1 receptor (TIR)-associated protein (TIRAP), TIR-domain-containing adaptor protein-inducing IFN-γ (TRIF) and TRIF-related adaptor molecule (TRAM), with TIR domains. These interactions trigger downstream signaling cascades leading to the activation of NF-κB, which controls the induction of pro-inflammatory cytokines and chemokines such as TNF-α, IL-1β, IL-6, IL-8, and IFN-γ [21]. Therefore, to suppress the inflammation cascade effectively, we hypothesized that blocking a point upstream of TLR4 signaling might be superior to blocking each mediator.

In the present study, TAK-242 effectively inhibited the nuclear translocation of NF-κB and the release of TNF-α, IL-1β, IL-6, KC, MIP-2 and IP-10 in the alveolar space in a dose-dependent manner. Although TAK-242 was reported

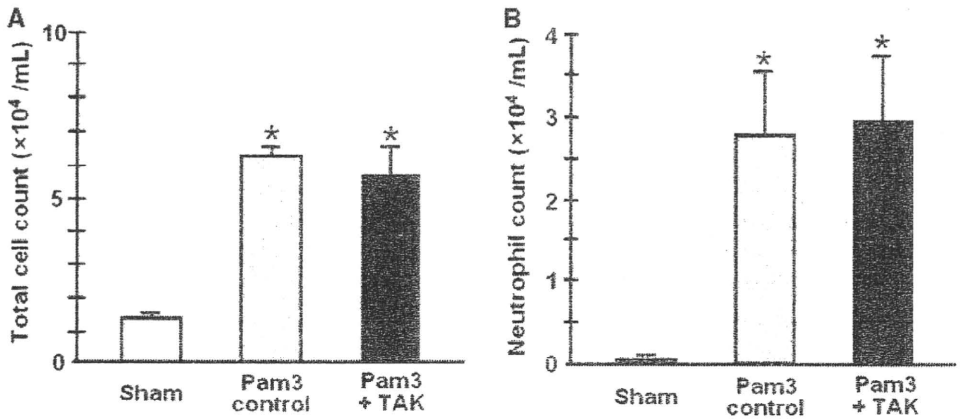


**Fig. 5** Pam3CSK4-induced inflammatory cell accumulations into the alveolar space. Mice received an intravenous injection of 3.0 mg/kg of TAK-242 or vehicle, followed by intratracheal administration of 2.5 mg/kg of Pam3CSK4 into the left lung; 6 h later, BAL fluid was obtained for a differential cell count. **a** Total cell counts in BAL fluid were not changed by treatment with TAK-242. **b** The recruitment of neutrophils into the alveolar space after Pam3CSK4 challenge did not differ between the groups. Values are the mean ± SE; $n = 4$–5 for each group. $^*P < 0.05$ compared with the sham group (*open bar*)

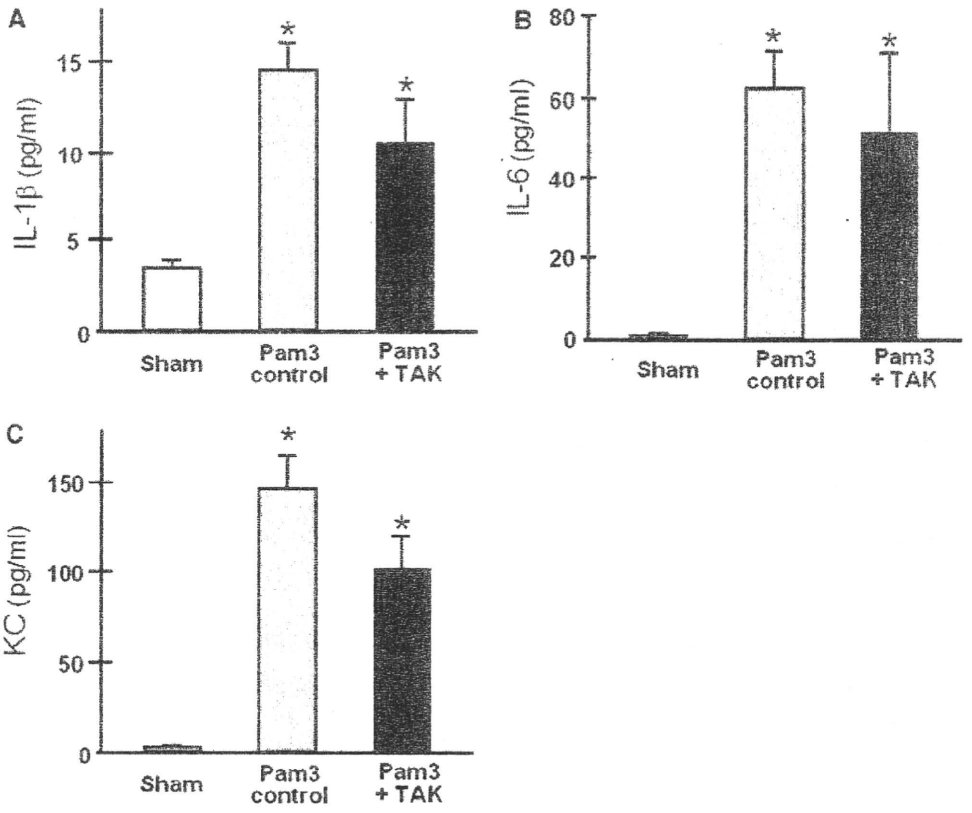


**Fig. 6** Cytokine and chemokine levels in BAL fluid following Pam3CSK4 challenge. Six hours after Pam3CSK4 instillation, BAL fluid was recovered and the levels of inflammatory mediators were measured. Pam3CSK4 induced significant upregulation of **a** IL-1$\beta$, **b** IL-6, and **c** KC. The elevation of these mediators was not inhibited by treatment with 3.0 mg/kg of TAK-242. Values are the mean ± SE; $n = 4$–5 for each group. $^*P < 0.05$ compared with the sham group (*open bar*)

to selectively suppress the TLR4 signal, commercial preparations of LPS may have contamination that could function as a TLR2 agonist [22, 23]. Therefore, we evaluate whether the inhibitory effects of TAK-242 were truly through inhibition of TLR4 signaling, using Pam3CSK4 that represents the N-terminal part of bacterial lipopeptide. Pam3CSK4, a potent activator of TLR2/TLR1, is known as an important tool for studying the TLR2-specific immune recognition mechanism because it is free of other contaminating bacterial components [24]. We observed that intratracheal challenge of Pam3CSK4 induced marked inflammatory cell accumulation and release of inflammatory mediators into the alveolar space. Since the TAK-242 treatment made no change in the Pam3CSK4-induced inflammatory response, we considered that the inhibitory effect of TAK-242 on LPS-induced lung injury could be through selective blockade of TLR4 signaling pathway.